Optimization of Structures and LJ Parameters of 1-Chloro-1,2,2-trifluorocyclobutane and 1,2-Dichlorohexafluorocyclobutane

Alexander C. Saladino[†] **and Pei Tang***[,†,‡]

Department of Anesthesiology and Department of Pharmacology, University of Pittsburgh School of Medicine, Pittsburgh, Pennsylvania 15261

Received: July 27, 2004; In Final Form: September 14, 2004

The structures and the Lennard-Jones (LJ) parameters of anesthetic 1-chloro-1,2,2-trifluorocyclobutane (**F3**) and nonimmobilizer 1,2-dichlorohexafluorocyclobutane (**F6**) were optimized by using ab initio calculations in conjunction with liquid and gas phase molecular dynamics simulations. Geometry optimization of various isomers of **F3** and **F6** was carried out with MP2/6-311+G(2d,p) that reproduced the experimental pucker angles of the precursors perfluorocyclobutane and cyclobutane more accurately than with B3LYP/6-311+G-(2d,p). Frequency calculations were performed to ensure that the optimized structures were at minimums of the potential energy surfaces. The partial atomic charges of **F3** and **F6** from the Merz−Singh−Kollman MP2/6-311+G(2d,p) calculations and the LJ parameters optimized previously for other halogenated compounds were used to start molecular dynamics simulations. The LJ parameters were then optimized through iterative adjustments to regenerate the heat of vaporization and the densities of **F3** and **F6** until the differences between the calculated values and the experimental values or empirical predicted values were less than 2%. With the optimized structures, the partial atomic charges, and the LJ parameters, **F3** and **F6** are readily usable as an anesthetic−nonimmobilizer pair in molecular dynamics simulations aimed at understanding the molecular mechanisms of general anesthesia.

Introduction

Inhaled anesthetics are an important class of drugs in producing general anesthesia, but the molecular mechanisms of their action in the central nervous system (CNS) remain elusive.[1] Some studies suggest that the pathways for the inhaled anesthetics to abolish (inhibit) the voluntary movement in response to noxious stimuli might be different from that of producing amnesia.[2] Whereas the former is believed to result from the depression of the spinal cord functions, the latter is presumptively mediated through possible molecular targets within the brain. Although the hypothesis of separate pathways for immobility and amnesia is not yet proven, compounds such as 1,2-dichlorohexafluorocyclobutane (**F6**), which can only impose amnesia but not immobility, have been identified and often refereed as nonimmobilizers.[3] These nonimmobilizers can be paired with structurally similar inhaled anesthetics that differ only by two or three atoms. By studying the interaction of the anesthetic−nonimmobilizer pairs with potential molecular targets, it is possible to elucidate the underlying mechanisms of the action of general anesthetics.[3−5]

Nonimmobilizer **F6** and anesthetic 1-chloro-1,2,2,-trifluorocyclobutane (**F3**) are a pair of cyclic halogenated compounds that have been well characterized experimentally.[3−6] Despite their structural resemblance (see Figure 1), they exhibit completely different anesthetic properties.[3] In model systems of biological membranes and proteins, many properties of **F3** and **F6** are also distinctly different. ^{19}F nuclear magnetic spectroscopy (NMR) studies showed that **F3** distributes preferentially

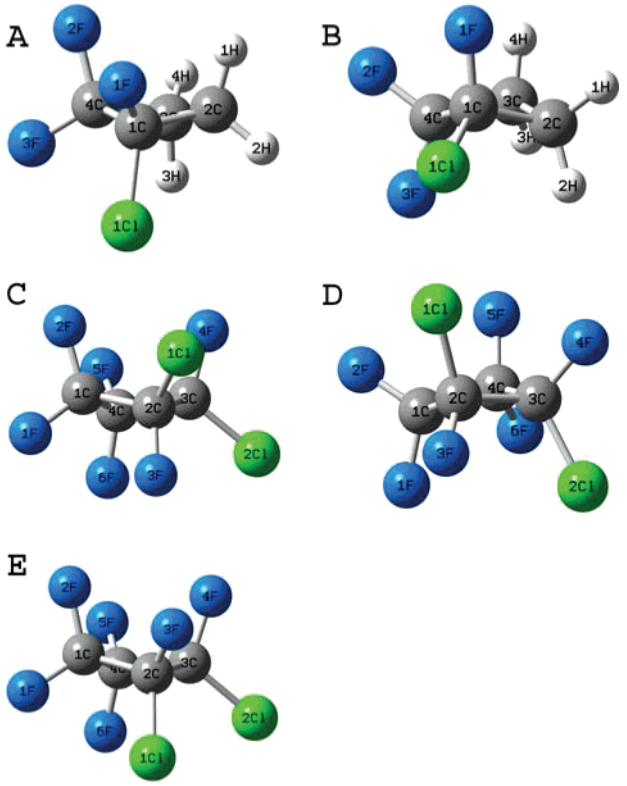

Figure 1. Molecular structures of (A) **F3** with axial Cl, (B) **F3** with equatorial Cl, (C) *trans*-**F6** with equatorial Cl; (D) *trans*-**F6** with axial Cl; and (E) *cis*-**F6**. The labeling conventions in the figures are also used in the text and tables.

* Address correspondence to this author. W-1357 Biomedical Science Tower, University of Pittsburgh School of Medicine, Pittsburgh, Pennsylvania 15261. Phone: (412) 383-9798. Fax: (412) 648-9587. E-mail: tangp@anes.upmc.edu.

[†] Department of Anesthesiology, University of Pittsburgh School of Medicine.

[‡] Department of Pharmacology, University of Pittsburgh School of Medicine.

10.1021/jp046662i CCC: $27.50
Published on Web 10/28/2004

into regions of the membrane that are water accessible; in contrast, **F6** solubilizes deeply into the lipid core.[4] The study concluded that although **F3** and **F6** show similar hydrophobicity in bulk solvents such as olive oil, their distributions in various regions in biomembranes might differ significantly. In the presence of transmembrane ion channels,[5] the ability of anesthetic **F3** to interact with the amphipathic residues near the membrane−water interface and the inability of nonimmobilizer **F6** to do the same may underline some of the most important characteristics of anesthetic−protein interactions that are of functional significance to general anesthesia. Exactly how and why **F3** and **F6** behave differently in biological systems is difficult to obtain in time-averaged experiments. Molecular dynamics (MD) simulations, in contrast, can provide very specific information about the differences in the molecular interactions and thus can facilitate a comprehensive understanding of the nature of anesthetic action.

Recent advancements in MD simulations have made it possible to characterize anesthetic interactions in membrane and with ion channels.[7−9] The nonbonded parameters of anesthetics and nonimmobilizers, especially their Lennard-Jones (LJ) parameters and atomic charges, are essential in MD simulations for quantifying dispersion/repulsion and electrostatic interactions that are responsible for many chemical and biological properties of the drug molecules. Although much effort has been devoted to developing and refining nonbonded parameters of anesthetics or nonimmobilizers,[10−13] the present study is the first attempt to optimize the structures and LJ parameters of the cyclic halogenated anesthetic and nonimmobilizer with a combined ab initio−empirical approach. The resultant structures, including various isomers of **F3** and **F6**, and the LJ parameters, are readily usable for applications of MD simulations involving these compounds.

Methods

Quantum Mechanics Calculations. All ab initio calculations were performed on Dell workstations with Gaussian03W.[14] Because of the availability of their experimental data, perfluorocyclobutane and cyclobutane were used as the structural precursors of **F3** and **F6** to evaluate the computational method. Geometry optimizations of perfluorocyclobutane and cyclobutane were performed with two levels of theory: a hybrid density functional theory B3LYP calculation[15,16] and a restricted Hartree−Fock calculation with a Moller−Plesset[17] second-order correlation energy correction (MP2),[18−22] both with the 6-311+G(2d,p) basis set.[23,24] The MP2/6-311+G(2d,p) methodology was used for the ab initio calculations of **F3** and **F6** since it produced more accurate results for perfluorocyclobutane than B3LYP/6-311+G(2d,p). All charge computations were performed with the Merz−Singh−Kollman scheme.[25,26] Frequency calculations, including the Gibbs free energy calculations, were performed on the structures optimized with the MP2/6-311+G(2d,p). The differences in the Gibbs free energy of the isomers were used to determine the isomeric ratios of axial to equatorial chlorines in **F3** or *trans*-**F6**, respectively:

$$\Delta G = -RT \ln K \tag{1}$$

where ΔG is the differences in the Gibbs free energy between the isomers, $R = 8.314$ J/(mol·K), T is the temperature, and K is the ratio of the isomers, [isomer A]/[isomer B].

Molecular Dynamic Simulations. All MD simulations were performed to optimize LJ parameters with NAMD version 2.5b1[27] on local SGI Octane workstations or on the Cray T3E at the Pittsburgh Supercomputer Center (PSC). For the pure liquid simulations, each system consisted of 125 molecules in a cubic cell whose starting density was similar to the experimental value of 1.3398 g/cm^3 for **F3** or 1.6443 g/cm^3 for **F6**. The cubic cell lengths were 28.18 and 30.86 Å for **F3** and **F6**, respectively. For gas-phase simulations, 11 molecules were placed in a box with a cubic cell length of 76.4 or 75.2 Å for **F3** or **F6**, respectively, so that the system was under the condition that approximately satisfied the idea gas law ($PV = nRT$). Different isomers were included in the simulation systems in the same ratio as calculated by the ab initio determined Gibbs free energy differences or based on experimental values.

The parameters for all energy terms, except for the nonbonded term, were adopted from CHARMM27.[28] The bonded forces were calculated at each time step (1 fs/step), the short-range nonbonded forces including the van der Waals and electrostatics interaction were computed every 2 time steps, and the long-range electrostatics forces were evaluated every 4 time steps. A smooth splitting function at a switch distance of 8.5 Å was used to separate the short-range component of electrostatic interactions from the long-range ones. The cutoff distance for the nonbonded interaction was 10 Å with the pair list distance extended to 12 Å. The pair list for the nonbonded interaction was recalculated every 20 steps, and the Particle Mesh Ewald (PME)[29] was used for calculating the long-range electrostatic forces. Periodic boundary conditions and molecule wrapping were employed. The Verlet integration algorithm[30,31] was used in every simulation.

Three different levels of simulations were performed for each system. An energy minimization with the conjugate gradient and line search algorithms was conducted for 10 ps (10 000 steps) to remove any bad contact points. The system was then simulated at constant moles, volume, and temperature (NVT) for 100 ps (100 000 steps) to ensure equilibrium. Langevin damping dynamics[32] was used to keep the temperature at a constant value. Finally, the system was simulated with constant moles, pressure, and temperature (NPT) for 1000 ps (1 000 000 steps). The Nosé−Hoover Langevin piston pressure control[33,34] and the Langevin damping dynamics were used to keep the pressure at 1 atm and the temperature at a desired constant, respectively. The chosen temperatures were 298 and 354 K for **F3**, and 290 and 333 K for **F6**, because of available information of the densities and the heats of vaporization at these temperatures.

The initial LJ parameters were estimated on the basis of the LJ parameters of halothane[10] and 1,1-difluoroethane[35] and refined with iterative simulations, in which adjustments of σ or ϵ values were repeated on the basis of comparisons between the simulation outputs with experimental data until the simulated density or the heat of vaporization was within 2% of experimental or empirically extrapolated "experimental" values, respectively. The heat of vaporization was evaluated with eq 2 based on the simulation-generated E_{gas} and E_{liq} values.

$$\Delta H_{vap} = E_{gas} - E_{liq} + RT \tag{2}$$

Results and Discussion

Geometry optimized **F3** and **F6**, including their isomers, are shown in Figure 1. The isomer of **F3** with axial chlorine has a lower Gibbs free energy and consequently higher population, which agrees well with previous experimental finding.[36] The resultant population percentages of **F3** isomers from eq 1 are 65% axial chlorine isomers and 35% equatorial chlorine isomers. There percentages were later implemented in both the liquid and gas-phase MD simulations. The percentages of three isomers

TABLE 1: Pucker Angles of Cyclobutane and Halogenated Cyclobutanes

molecule	B3LYP	MP2	exptl
cyclobutane	26	31	27,[a] 28,[b] 31,[c] 35[d]
perfluorocyclobutane	11	22	17,[e] 20,[f] 23,[g] 24[h]
F3, axial		28	
F3, equatorial		29	
F6, cis		25	
F6, trans			
axial		22	
equatorial		27	

[a] Reference 47. [b] Reference 38. [c] Reference 37. [d] Reference 48. [e] Reference 49. [f] Reference 50. [g] Reference 39. [h] Reference 40.

of **F6**, including cis and trans with axial and equatorial chlorine positions, were obtained in a similar fashion. The isomer distribution of **F6** used in MD simulations was 54% cis-isomer, 27% trans-isomers with equatorial chlorines, and 19% trans-isomers with axial chlorines.

Because of the nature of cyclic four-membered compounds, the ability to accurately predict the nonplanarity of the carbon ring became one of the central criteria in determining the computation method for the geometry optimizations of these compounds. As shown in Table 1, the MP2/6-311+G(2d,p) and the B3LYP/6-311+G(2d,p) performed equally well on the geometry optimization of cyclobutane, as indicated by well matched pucker angles from the calculations and the experiments. Severe deviation from the experimental values, however, became apparent when the B3LYP/6-311+G(2d,p) was used for the calculations of perfluorocyclobutane. In contrast, the MP2/6-311+G(2d,p) calculations on perfluorocyclobutane produced a dihedral angle of the ring of 22°, well within the experimentally measured range.[37−43] The different performance of B3LYP and MP2 on fluorinated cyclic compounds can probably be attributed to their different efficiency in treating the long-range dispersion interactions. Nevertheless, the choice of the MP2/6-311+G(2d,p) seems more favorable for **F3** and **F6**, in which halogen atoms are involved. On average the pucker angles of **F3** are greater than those of **F6** (see Table 1), indicating that the ring has a propensity to be less puckering when more heavy atoms are present. For the same reason, the frequency of the puckering mode for perfluorocyclobutane was found to be much lower than that of cyclobutane.[43]

Other geometry parameters are summarized in Table 2. The closest experimental geometric parameters that could be compared with those of **F3** and **F6** were from chlorocyclobutane[44] and perfluorocyclobutane.[39] For clarity, only weighted averaged values of different isomers are presented. The calculated axial C−X bonds of **F3** and **F6** are in general longer than the corresponding equatorial bonds. The same characteristics were also found from the IR and Raman spectra.[36] The overall good agreement between calculated and referenced experimental results suggests that the optimized geometries are accurate. The coordinates of the optimized structures will be provided in the Supporting Information.

Table 3 summarizes the partial atomic charges of **F3** and **F6** derived from the electrostatic potential (ESP) with use of the Merz−Singh−Kollman scheme. The variations of charge values in different isomers are in general small but often significant. Therefore, the distinct charge assignments for different isomers were later used in the condensed phase MD simulations. One may notice that large negative partial charges are assigned to C3 of **F3**, resulting from the polarization by the adjacent highly positively charged C4. Averaged dipole moments calculated from the ESP charges are 3.17 and 0.78 for **F3** and **F6**, respectively.

TABLE 2: Optimized Bond Lengths (Å) and Angles (deg) of F3 and F6

	F3	**F6**	exptl
C−H[b]	1.087		1.09[c]
C−H[a]	1.090		1.09[c]
C−F[b]	1.347	1.335	1.333[d]
C−F[a]	1.362	1.346	1.333[d]
C−Cl[b]	1.758	1.738	(1.70, 1.72)[e]
C−Cl[a]	1.775	1.749	(1.77, 1.76, 1.75)[e]
C−C	1.542	1.561	1.550,[f] 1.566[d]
C−C−H[b]	116.7		115[g]
C−C−H[a]	111.1		114[g]
C−C−F[b]	118.1	116.3	117.5[d]
C−C−F[a]	110.2	110.5	110.6[d]
C−C−Cl[b]	119.6	119.0	
C−C−Cl[a]	112.0	113.4	
C−C−C−Cl[a]	93.1	97.6	117[f]
C−C−C−Cl[b]	143.4	140.7	132[f]
C−C−C	88.2	88.6	89.3[d]
H−C−H	111.2		114,[c] 110[g]
F−C−F	108.0	110.1	109.9[d]
Cl−C−F	109.7	111.2	

[a] Axial. [b] Equatorial. [c] Reference 50. [d] Reference 49. [e] Reference 51. [f] Reference 44. [g] Reference 52.

TABLE 3: Assignment of Partial Atomic Charges (ESP) for Various Conformations of F3 and F6

F3			**F6**			
	q(e$^-$)			q(e$^-$)		
					trans	
atomic center	equatorial Cl	axial Cl	atomic center	cis	axial Cl	equatorial Cl
C1	0.03	0.11	C1	0.46	0.38	0.43
C2	−0.07	−0.09	C2	0.03	0.04	−0.01
C3	−0.27	−0.26	C3	0.09	0.03	−0.05
C4	0.56	0.49	C4	0.34	0.48	0.46
F1	−0.15	−0.16	F1	−0.18	−0.18	−0.16
F2	−0.23	−0.21	F2	−0.18	−0.18	−0.19
F3	−0.24	−0.23	F3	−0.09	−0.11	−0.11
Cl1	−0.06	−0.07	F4	−0.13	−0.11	−0.11
H1	0.08	0.10	F5	−0.14	−0.20	−0.16
H2	0.12	0.08	F6	−0.19	−0.20	−0.20
H3	0.12	0.11	Cl1	−0.01	0.02	0.05
H4	0.11	0.13	Cl2	0.00	0.02	0.05

TABLE 4: Condensed Phase Properties of F3 and F6

		ΔH_{vap} (kJ/mol)		density (g/cm^3)	
	temp (K)	calcd	exptl	calcd	exptl
F3	298			1.32	1.34[b]
	354	30.9	30.8[a]		
F6	290			1.62	1.64[b]
	333	28.4	28.9[a]		

[a] From ACD Software V4.67 via SciFinder. [b] Reference 53.

The condensed phase properties of **F3** and **F6**, including the experimentally determined liquid densities and the experimentally derived empirical predictions of the heats of vaporization from the Advance Chemistry Development (ACD) software, were used as references for measuring the quality of LJ parameters for **F3** and **F6**. As shown in Table 4, the calculated heats of vaporization from eq 2 on the basis of simulated E_{liq} and E_{gas} well reproduced experimental values after more than 10 iterations of MD simulations for each compound. The differences between the calculated and experimental heats of vaporization and liquid densities are less than 2% for both **F3** and **F6** when the finalized LJ parameters in Table 5 were used.

One may notice that the σ values of the carbons attached to F in **F3** (i.e., C2 and C3) are smaller than those in **F6**, but their corresponding ϵ values are in an opposite trend. The differences

TABLE 5: Lennard-Jones Parameters of F3 and F6

F3			F6		
atomic center	σ(Å)[a]	ϵ (kcal/mol)[a]	atomic center	σ(Å)[a]	ϵ (kcal/mol)[a]
C1	3.52	0.075	C1	3.78	0.046
C2	3.89	0.055	C2	3.78	0.046
C3	3.89	0.055	C3	3.78	0.046
C4	3.52	0.075	C4	3.78	0.046
F1	2.83	0.095	F1	2.98	0.078
F2	2.83	0.095	F2	2.98	0.078
F3	2.83	0.095	F3	2.98	0.078
Cl1	3.49	0.267	F4	2.98	0.078
H1	2.35	0.022	F5	2.98	0.078
H2	2.35	0.022	F6	2.98	0.078
H3	2.35	0.022	Cl1	3.50	0.254
H4	2.35	0.022	Cl2	3.50	0.254

[a] Combination rule: $\sigma_{12} = (\sigma_1 + \sigma_2)/2$; $\epsilon_{12} = \sqrt{\epsilon_1 * \epsilon_2}$.

between the equivalent σ or ϵ values of F and Cl atoms in **F3** and **F6** are also discernible but on a smaller scale. Similar changes in LJ parameters were also noticed in our previous study[10] on a pair of linear molecules: anesthetic halothane (CF_3-CHClBr) and its nonanesthetic analogue C_2F_6, where atoms in halothane have smaller σ and greater ϵ values than the corresponding atoms in C_2F_6. Nevertheless, the transferability of LJ parameters between anesthetic and nonanesthetic molecules is poor, which might result directly from the lower symmetry and higher dipole moment of anesthetic molecules as compared to their nonanesthetic analogues. It is, therefore, important to use specific LJ parameters for these molecules in any MD simulations that are intended to accurately simulate anesthetic effects on a biological system.

Most prior LJ parameters for halogenated molecules were developed on either linear or branched molecules.[10,45,46] If these parameters are adopted directly for cyclic compounds, such as **F3** and **F6**, they often fail to reproduce the condensed phase properties of these compounds properly. In the case of **F3** and **F6**, their heats of vaporization and densities could deviate from the experimental data significantly if generic parameters are used. Similarly, unsigned error of perfluorocyclobutane was found to be higher than those of linear fluorinated compounds when the generalized LJ parameters for perfluoroalkanes were used.[46] Thus, it is not surprising that the transferability of the existing LJ parameters to cyclic compounds is limited because most of the parameters were developed on small linear fluoroethanes.

In summary, the optimized parameters of **F3** and **F6** from this study are in excellent accord with experimental results. These parameters are ready to be implemented in MD simulations that may involve **F3** and **F6**. These molecules can be used either as molecular probes in searching for a better molecular understanding of the mechanisms of general anesthesia or as a pair of cyclic halogenated compounds for other interesting scientific exploration.

Acknowledgment. The authors thank Professor Yan Xu and Dr. Zhanwu Liu for stimulating discussions. The research was facilitated through an allocation of advanced computing resources at the Pittsburgh Supercomputing Center through the support of the National Science Foundation and the Commonwealth of Pennsylvania. This research was supported by a grant from the NIH (R01GM66358).

Supporting Information Available: The optimized Cartesian coordinates in standard orientation of 1-chloro-1,2,2-trifluorocyclobutane (**F3**) and 1,2-dichlorohexafluorocyclobutane (**F6**). This material is available free of charge via the Internet at http://pubs.acs.org.

References and Notes

(1) Campagna, J. A.; Miller, K. W.; Forman, S. A. *N. Engl. J. Med.* **2003**, *348*, 2110.
(2) Eger, E. I., 2nd; Koblin, D. D.; Harris, R. A.; Kendig, J. J.; Pohorille, A.; Halsey, M. J.; Trudell, J. R. *Anesth. Analg.* (*Baltimore*) **1997**, *84*, 915.
(3) Koblin, D. D.; Chortkoff, B. S.; Laster, M. J.; Eger, E. I. n.; Halsey, M. J.; Ionescu, P. *Anesth. Analg.* (*Baltimore*) **1994**, *79*, 1043.
(4) Tang, P.; Yan, B.; Xu, Y. *Biophys. J.* **1997**, *72*, 1676.
(5) Tang, P.; Hu, J.; Liachenko, S.; Xu, Y. *Biophys. J.* **1999**, *77*, 739.
(6) Forman, S. A. *Toxicol. Lett.* **1998**, *100*−*101*, 169.
(7) Tang, P.; Xu, Y. *Proc. Natl. Acad. Sci. U.S.A.* **2002**, *99*, 16035.
(8) Koubi, L.; Tarek, M.; Bandyopadhyay, S.; Klein, M. L.; Scharf, D. *Biophys. J.* **2001**, *81*, 3339.
(9) Koubi, L.; Tarek, M.; Bandyopadhyay, S.; Klein, M. L.; Scharf, D. *Anesthesiology* **2002**, *97*, 848.
(10) Liu, Z. W.; Xu, Y.; Saladino, A. C.; Wymore, T.; Tang, P. *J. Phys. Chem. A* **2004**, *108*, 781.
(11) Tang, P.; Zubryzcki, I.; Xu, Y. *J. Comput. Chem.* **2001**, *22*, 436.
(12) Scharf, D.; Laasonen, K. *Chem. Phys. Lett.* **1996**, *258*, 276.
(13) Pohorille, A.; Wilson, M. A. *J. Chem. Phys.* **1996**, *104*, 3760.
(14) Frisch, M. J.; Trucks, G. W.; Schlegel, H. B.; Scuseria, G. E.; Robb, M. A.; Cheeseman, J. R.; Montgomery, J. A., Jr.; Vreven, T.; Kudin, K. N.; Burant, J. C.; Millam, J. M.; Iyengar, S. S.; Tomasi, J.; Barone, V.; Mennucci, B.; Cossi, M.; Scalmani, G.; Rega, N.; Petersson, G. A.; Nakatsuji, H.; Hada, M.; Ehara, M.; Toyota, K.; Fukuda, R.; Hasegawa, J.; Ishida, M.; Nakajima, T.; Honda, Y.; Kitao, O.; Nakai, H.; Klene, M.; Li, X.; Knox, J. E.; Hratchian, H. P.; Cross, J. B.; Adamo, C.; Jaramillo, J.; Gomperts, R.; Stratmann, R. E.; Yazyev, O.; Austin, A. J.; Cammi, R.; Pomelli, C.; Ochterski, J. W.; Ayala, P. Y.; Morokuma, K.; Voth, G. A.; Salvador, P.; Dannenberg, J. J.; Zakrzewski, V. G.; Dapprich, S.; Daniels, A. D.; Strain, M. C.; Farkas, O.; Malick, D. K.; Rabuck, A. D.; Raghavachari, K.; Foresman, J. B.; Ortiz, J. V.; Cui, Q.; Baboul, A. G.; Clifford, S.; Cioslowski, J.; Stefanov, B. B.; Liu, G.; Liashenko, A.; Piskorz, P.; Komaromi, I.; Martin, R. L.; Fox, D. J.; Keith, T.; Al-Laham, M. A.; Peng, C. Y.; Nanayakkara, A.; Challacombe, M.; Gill, P. M. W.; Johnson, B.; Chen, W.; Wong, M. W.; Gonzalez, C.; Pople, J. A. *Gaussian 03*, revision B.01; Gaussian, Inc.: Pittsburgh, PA, 2003.
(15) Lee, C.; Yang, W.; Parr, R. G. *Phys. Rev. B* **1988**, *37*, 785.
(16) Becke, A. D. *J. Chem. Phys.* **1993**, *98*, 5648.
(17) Moller, C.; Plesset, M. S. *Phys. Rev.* **1934**, *46*, 618.
(18) Frisch, M. J.; Head-Gordon, M.; Pople, J. A. *Chem. Phys. Lett.* **1990**, *166*, 275.
(19) Frisch, M. J.; Head-Gordon, M.; Pople, J. A. *Chem. Phys. Lett.* **1990**, *166*, 281.
(20) Head-Gordon, M.; Pople, J. A.; Frisch, M. J. *Chem. Phys. Lett.* **1988**, *153*, 503.
(21) Head-Gordon, M.; Head-Gordon, T. *Chem. Phys. Lett.* **1994**, *220*, 122.
(22) Saebo, S.; Almlof, J. *Chem. Phys. Lett.* **1989**, *154*, 83.
(23) McLean, A. D.; Chandler, G. S. *J. Chem. Phys.* **1980**, *72*, 5639.
(24) Krishnan, R.; Binkley, J. S.; Seeger, R.; Pople, J. A. *J. Chem. Phys.* **1980**, *72*, 650.
(25) Singh, U. C.; Kollman, P. A. *J. Comput. Chem.* **1984**, *5*, 129.
(26) Besler, B. H.; Merz, K. M., Jr.; Kollman, P. A. *J. Comput. Chem.* **1990**, *11*, 431.
(27) Kale, L.; Skeel, R.; Bhandarkar, M.; Brunner, R.; Gursoy, A.; Krawetz, N.; Phillips, J.; Shinozaki, A.; Varadarajan, K.; Schulten, K. *J. Comput. Phys.* **1999**, *151*, 283.
(28) MacKerell, A. D. *Abstr. Pap. Am. Chem. Soc.* **1998**, *216*, 042.
(29) Darden, T.; York, D.; Pedersen, L. *J. Chem. Phys.* **1993**, *98*, 10089.
(30) Allen, M. P.; Tildesley, D. J. *Computer Simulation of Liquids*; Oxford University Press: New York, 1987.
(31) Verlet, L. *Phys. Rev.* **1967**, *159*, 98.
(32) Brünger, A. X-PLOR, Version 3.1: A system for X-ray crystallography and NMR; Yale University: New Haven, CT, 1992.
(33) Hoover, W. G. *Phys. Rev. A* **1985**, *31*, 1695.
(34) Nose, S. *J. Chem. Phys.* **1984**, *81*, 511.
(35) Chen, I. J.; Yin, D. X.; MacKerell, A. D. *J. Comput. Chem.* **2002**, *23*, 199.
(36) Powell, D. L.; Gatial, A.; Klaeboe, P.; Nielsen, C. J.; Kondow, A. J. *J. Mol. Struct.* **1993**, *300*, 209.
(37) Stein, A.; Lehmann, C. W.; Luger, P. *J. Am. Chem. Soc.* **1992**, *114*, 7684.
(38) Egawa, T.; Fukuyama, T.; Yamamoto, S.; Takabayashi, F.; Kambara, H.; Ueda, T.; Kuchitsu, K. *J. Chem. Phys.* **1987**, *86*, 6018.
(39) Beagley, B.; Calladine, R.; Pritchard, R. G.; Taylor, S. F. *J. Mol. Struct.* **1987**, *158*, 309.
(40) Alekseev, N. V.; Barzdain, P. P. *Zh. Strukt. Khim.* **1974**, *15*, 181.

(41) Lemaire, H. P.; Livingston, R. L. *J. Am. Chem. Soc.* **1952**, *74*, 5732.
(42) Henseler, D.; Hohlneicher, G. *J. Phys. Chem. A* **1998**, *102*, 10828.
(43) Fischer, G.; Purchase, R. L.; Smith, D. M. *J. Mol. Struct.* **1997**, *405*, 159.
(44) Jonvik, T. *J. Mol. Struct.* **1988**, *172*, 213.
(45) Chipot, C.; Wilson, M. A.; Pohorille, A. *J. Phys. Chem. B* **1997**, *101*, 782.
(46) Watkins, E. K.; Jorgensen, W. L. *J. Phys. Chem. A* **2001**, *105*, 4118.
(47) Meiboom, S.; Snyder, L. C. *J. Chem. Phys.* **1970**, *52*, 3857.
(48) Meiboom, S.; Snyder, L. C. *J. Am. Chem. Soc.* **1967**, *89*, 1038.
(49) Chang, C.-H.; Porter, R. F.; Bauer, S. H. *J. Mol. Struct.* **1971**, *7*, 89.
(50) Dunitz, J. D.; Schomaker, V. *J. Chem. Phys.* **1952**, *20*, 1703.
(51) Margulis, T. N. *Acta Crystallogr.* **1965**, *19*, 857.
(52) Kim, H.; Gwinn, W. D. *J. Chem. Phys.* **1965**, *44*, 865.
(53) PCR Research Chemicals Catalog 1994−1995; PCR Inc.: Gainesville, FL, 1994.